HHS Public Access

Author manuscript

Biol Psychiatry. Author manuscript; available in PMC 2022 May 15.

Published in final edited form as:

Biol Psychiatry. 2021 May 15; 89(10): 947–958. doi:10.1016/j.biopsych.2020.12.004.

Heroin Seeking and Extinction from Seeking Activate Matrix Metalloproteinases at Synapses on Distinct Subpopulations of Accumbens Cells

Vivian C. Chioma[1], **Anna Kruyer**[1], **Ana-Clara Bobadilla**[1,2], **Ariana Angelis**[1], **Zachary Ellison**[1], **Ritchy Hodebourg**[1], **Michael D. Scofield**[1,3], **Peter W. Kalivas**[*,1]

[1]Department of Neuroscience, Medical University of South Carolina, Charleston, SC, USA, 29425

[2]School of Pharmacy, University of Wyoming, Laramie, Wyoming, USA, 82701

[3]Department of Anesthesia and Perioperative Medicine, Medical University of South Carolina, Charleston, SC, USA, 29425

Abstract

Background: Seeking addictive drugs is regulated by synaptic plasticity in the nucleus accumbens core and involves distinct plasticity in D1- and D2-medium spiny neurons (MSNs). However, it is unknown how differential plasticity between the two cell-types is coordinated. Synaptic plasticity and seeking behavior induced by drug-paired cues depends on plasticity not only in the canonical pre- and post-synapse, but also on cue-induced changes in astrocytes and the extracellular matrix adjacent to the synapse. Drug cue-induced signaling in the extracellular matrix is regulated by catalytic activity of matrix metalloproteases-2,9 (MMP-2,9). We hypothesized that the cell-type specific synaptic plasticity is associated with parallel cell-specific activity of MMP-2 and MMP-9.

Methods: Transgenic rats were trained on a heroin self-administration protocol followed by two weeks of drug withdrawal, and a light/tone cue was paired with heroin delivery. Confocal microscopy was used to make morphological measurements in membrane reporter-transduced D1- and D2-MSNs and astrocytes, and MMP-2,9 gelatinase activity adjacent to cell surfaces was quantified using in vivo zymography.

Results: Presenting heroin-paired cues transiently increased MMP-9 activity around D1-MSN dendritic spines and synapse-proximal astroglial processes. Conversely, extinction training induced long-lasting increases in MMP-2 activity adjacent to D2-MSN synapses. Moreover, heroin-paired cues increased tissue inhibitor of metalloproteinases-1,2, which caused transient inhibition of MMP-2 activity around D2-MSNs during cue-induced heroin seeking.

[*]Corresponding author: Peter Kalivas, Medical University of South Carolina, 173 Ashley Ave., BSB 403- MSC 510, Charleston, SC 29425, kalivasp@musc.edu.

Author Contributions

V.C.C. and P.W.K. designed and planned the experiments. V.C.C., A.K., A-C.B., R.H., A.A., and Z.E. performed the behavioral experiments and collected the behavioral and imaging data. V.C.C., A.K. and P.W.K analyzed and interpreted the data. V.C.C. and M.D.S. developed Imaris MMP dendritic subcompartment and punctate signal localization analysis. V.C.C. and P.W.K. wrote the manuscript with editorial comments from all authors.

Disclosures

The authors have no disclosures and declare no competing interests.

Conclusions: The differential regulation of heroin seeking and and extinguished seeking by different MMP subtypes on distinct cell populations poses MMP-2,9 activity as an important mediator and contributor in heroin-induced cell-specific synaptic plasticity.

Keywords

matrix metalloprotease; accumbens; heroin; medium spiny neuron; astroglia; TIMP

Introduction

Opioids are a leading cause of substance use disorder (SUD) and drug overdose-related deaths (1). In animal models and humans, opioid use induces enduring and transient synaptic plasticity in glutamatergic cortico-striatal circuits that contribute to great difficulty in managing relapse in Opioid Use Disorder (OUD), (2, 3). The nucleus accumbens core (NAcore) subcompartment of the ventral striatum is a center for initiating motivated behaviors, and harbors many synaptic adaptations supporting opioid seeking (3–7). Synaptic adaptations are also produced in NAcore when rodents are trained to extinguish drug seeking in a drug-associated context (8).

Drug seeking and extinction of seeking are regulated differently by NAcore neuron subtypes. Activating D1-expressing GABAergic medium spiny neurons (D1-MSNs) promotes drug seeking, while D2-MSN stimulation promotes reduced drug seeking in drug-associated contexts after extinction training (9, 10). In parallel with the involvement of distinct subtypes, drug seeking produces synaptic plasticity primarily in D1-MSNs, and extinction training causes synaptic adaptations in D2-MSNs (8, 11, 12).

Although differential roles by D1- and D2-MSNs in motivated behaviors is supported by substantial literature, it remains unclear how the induction of differential synaptic plasticity in the two cell-types is managed at a cellular level. However, drug-associated synaptic plasticity in NAcore depends not only on pre- and postsynaptic signaling, but also on signaling in perisynaptic astroglial processes and the adjacent extracellular matrix (ECM) (13, 14). For example, enduring retraction of astroglial processes from synapses occur after extinction training (15–18), while re-association of astroglial processes with synapses and activation of ECM signaling occur during cue-induced drug seeking (16, 17, 19).

Signaling in the ECM is regulated by the gelatinase family of matrix metalloproteases (MMP-2,9) (20, 21) and endogenous tissue inhibitors of metalloproteinases (TIMP-1,2). Activating MMP-9 is necessary for classic forms of synaptic plasticity, such as hippocampal long-term potentiation (20, 22, 23), and MMP-9 activation is necessary for both drug cue-induced transient synaptic plasticity (17, 24, 25) and alcohol and cocaine seeking (26, 27). However, drug seeking changes in MMP-2,9 and TIMP-1,2 activity have not been mapped onto the different cell-types in NAcore known to mediate different addictive behaviors. Here we evaluate the hypothesis that different MMPs and/or TIMPs activate around different NAcore cell types (D1-MSN, D2-MSN or astroglia) during cue-induced heroin seeking and after extinction training from heroin seeking.

Methods

Animals, Housing and Surgery

Ninety-seven male and female Long Evans D1 and D2-Cre (+) transgenic rats (cre recombinase under control of the dopamine receptor D1 or D2 promoter (28)) and 41 Cre (−) wildtype littermates were individually housed in a climate-controlled environment using a 12:12 hr dark/light cycle with food and water made available ad libitum. Experimentation occurred during the dark phase. All procedures were conducted in accordance with the NIH Guide for the Care and Use of Laboratory Animals and the Assessment and Accreditation of Laboratory Animal Care.

Drugs and reagents

Heroin HCl (NIDA), was dissolved in sterile saline. TIMP-1 and −2 antibodies (R&D Systems, #AF970 and #AF971, respectively) or normal Goat IgG (R&D Systems, #AB-108-C) were microinjected (29, 30). MMP-2i (Millipore-Sigma, #444288(31)) and MMP-9i (Millipore-Sigma, #444278(32)) were dissolved in 1% DMSO. Dye-quenched fluorescein conjugate gelatin (Thermo Fisher Scientific, #D12054; 1 mg/ml in PBS; 1.5 μl/hemisphere) was used for *in vivo* zymography. D1- and D2-MSNs were virally transfected with AAV1-EF1a-dflox-hChR2-mCherry (Addgene). Astroglia were selectively labeled using a glia fibrillary acidic protein promoter with AAV5-GFAP-hM3dq-mCherry (Zurich University, Switzerland).

Heroin Self-administration, Withdrawal Period, and Cued Reinstatement

Rats underwent daily 3-hour yoked-saline or heroin self-administration sessions in two-lever operant chambers (Med Associates). Active lever presses delivered 100 μg (days 1–2), 50 μg (days 3–4), or 25 μg (days 5–10) per IV infusion of heroin (FR1) paired with cues (light and tone) followed by a 20s timeout (33). Rats self-administered heroin for 10 days reaching criteria of ≥10 infusions/day on the last 3 days, followed by withdrawal period (with or without extinction training) of 10 days or until extinction-trained rats emitted ≤25 active presses for two consecutive days. Tissue collection occurred 24 hours after last day of extinction or abstinence, during an extinction session (15 min) or a cued reinstatement test (15 or 120 mins).

In vivo zymography

I*n vivo* zymography was utilized to assess changes in MMP-2,9 activity (17). Dye-quenched FITC-gelatin was microinjected (ThermoFisher Scientific; in 1 mg/mL PBS, pH 7.2–7.4; 1.5μl/side) (17), and 15 min later rats were transcardially perfused with 4% paraformaldehyde. Thus, for 15 min time points rats were microinjected 15 min prior to being placed in the operant chamber, and for the 120 min time point, rats were microinjected 105 min after beginning their operant session. Only slices containing both the anterior commissure (landmark for NAcore) and injection site were imaged and analyzed (ImageJ, NIMH, Bethesda, MD). Integrated densities were averaged over 4–7 sections/rat and normalized to yoked-saline control values.

Immunohistochemistry

Tissue sections were obtained and incubated in PBS+Triton-X100, then blocked with PBS+Triton-X100 with 2% normal goat serum. Primary antibodies against mCherry (Rb anti-dsRed, 1:500; Takara #632496 or Mouse anti-mCherry, 1:1000; LSBio #204825), TIMP-1 (1:500; Abcam #18352) and TIMP-2 (1:200; Thermo Fisher Scientific #12207) were incubated for 48 hours at 4°C. Tissue virally transfected with GFAP-mCherry virus were incubated with synapsin I antibody (1:1000; Abcam #64581). Following incubation with primary antibodies, slices were incubated in species-specific fluorescent secondary antibodies (Alexa Fluor; 1:1000; ThermoFisher Scientific).

Confocal Microscopy Imaging and Quantification

Z-stacks were acquired using a Leica SP5 (Wetzlar, Germany) or Zeiss LSM 880 (Oberkochen, Germany) laser scanning confocal microscope. Previously reported criteria for dendritic spine morphology (34) and astroglial (16) image acquisition were applied. Using Imaris Surface module, mCherry-labeled dendritic segments were cropped and isolated from background. The region within 300nm from the surface of each dendritic segment was used to mask MMP-2,9 gelatinolytic puncta. Puncta were isolated around the region of interest using intensity-based thresholding (Figure 1F–K). MMP gelatinolytic activity localized adjacent to the dendrite was calculated by dividing volume (μm^3) of MMP puncta by volume (μm^3) of 300nm-expanded region around the dendrite. This same approach was employed to quantify extracellular TIMP-1,2 expression around D1- and D2-MSNs. To quantify dendritic spine head diameter the Filament module was used to trace the dendritic shaft and dendritic spines, and create dendritic subcompartments to quantify MMP-2,9 puncta around spine heads versus shaft (35). The digital astroglial model generated from the hM3Dq-mCherry signal is described elsewhere (15, 36) and was used to mask out MMP-2,9 activity and Synapsin I signal that were not co-registered within 300nm the astroglial volume.

Statistical analysis

All statistical analyses were conducted using GraphPad (Prism v8). Behavioral data were analyzed by two-way ANOVA followed by Sidak post hoc. D'Agostino-Pearson normality test was used to determine if data were normally distributed. Kruskal-Wallis with Dunn's post hoc comparisons or Mann-Whitney tests were used when one or more treatment groups were found not normally distributed. Data found normally distributed were analyzed using a one- or two-way ANOVA. All D1/D2 cell-specific data was analyzed using Nested t-test (two group comparison) or Nested ANOVA with post-hoc Sidak post hoc. In all cases, p values <0.05 were considered significant. All data except behavior was collected and analyzed by investigators blind to animal treatment groups.

Results

Heroin self-administration, extinction and cued heroin seeking

Rats were trained to self-administer yoked-saline or heroin for 10 days and subsequently withdrawn for 10 days (extinguished or home-cage abstinence) (Figure 1A). There were no sex or genotypic differences in heroin self-administration between D1/D2-Cre rats (Figure

1B,C; Figure S1A–C). After extinction training, rats were returned to operant environment for one of three behavioral tests: 1) refraining (returned to the extinguished context for 15 min with no cues), 2) 15 min of cue-induced seeking, or 3) 120 min of cued seeking. The D1- and D2-Cre genotypes, and males and females exhibited equivalent increases in heroin seeking (active lever pressing) in response to heroin-paired cues for 15 or 120 min compared to the average responding during the last 2 days of extinction or the 15 min refraining session (Figure 1D,E; S1G,H). Also, both genotypes had extinguished cue-induced active lever pressing by the last 15 min of the 120 min reinstatement session (Fig S1D). No genotypic or sex differences were observed in inactive lever pressing after 15 or 120 min of cued reinstatement (Figure S1E–H).

MMP-2 and −9 activity localizes differently around D1- and D2-MSNs during heroin seeking and extinguished responding

Male and female D1- and D2-Cre rats were transduced with a Cre-dependent mCherry reporter and *in vivo* zymography used to assess MMP-2,9 proteolytic activity. FITC-quenched gelatin was bilaterally microinjected into NAcore 24 hours after the last day of withdrawal (with or without extinction training) or immediately prior to behavioral testing. Baseline MMP-2,9 activity was obtained from yoked-saline rats sacrificed 24 hours after last withdrawal day. NAcore MMP-2,9 activity quantified at low magnification (Figure S2A) was increased only in cue-induced heroin seeking rats (Figure S2B), and there was no difference across groups between D1- and D2-cre rats (Figure S2C–E).

The workflow for assessing cell-type specific MMP-2,9 proteolytic activity is shown in Figure 1F–J (Figure 1K). We observed increased MMP-2,9 gelatinolytic puncta localized within 300nm of D1-MSN dendritic surfaces in cue-reinstated rats (15 min) compared to yoked-saline or extinguished rats, and there was no difference between rats withdrawn with or without extinction training (Figure 2A,B). MMP-2,9 activity was reduced below baseline extinction levels after 15 min in an extinction trial (refraining), or after rats had undergone within trial extinction (Figure S1D) after 120 min of cued reinstatement. Thus, increased MMP-2,9 activity was initiated by heroin-paired cues around D1-MSN dendrites, and was reduced by refraining during extinction.

MMP-2,9 gelatinolytic activity proximal to D2-MSN dendrites in NAcore was increased by extinction training to levels greater than either yoked-saline or abstinent withdrawn rats (Figure 2C,D). Thus, only rats withdrawn and undergoing daily extinction training show elevated MMP-2,9 around D2-MSNs. Exposing rats to 15 min in an extinguished context (refraining) did not alter the extinction training-induced increase in MMP-2,9 activity. In contrast, presenting heroin cues for 15 min reversed the extinction-induced increased MMP-2,9 activity to levels equivalent to yoked-saline or abstinent rats. This reduction was transient since MMP-2,9 activity around D2-MSN dendrites was restored to extinction levels by 120 min in cued reinstatement when rats had undergone within trial extinction. Importantly, there was no difference in total MMP activity normalized to the volume of the image series across treatment groups between D1 and D2 MSN cell-types, supporting cell-specific differences within 300nm of the dendrite surface (Figure S2E). Also, we randomly sampled D1 MSN dendrites after 15 min of cued reinstatement, and

there was minimal intracellular MMP-2,9 activity detected inside the dendrite (Figure S2F), indicating that the cue-induced increases were selective for the extracellular compartment. We additionally performed a two-way ANOVA to identify a main effect difference between D1- and D2-MSNs ($F_{(1,304)}$=4.24, p=0.040).

MMP gelatinolytic activity enrichment around dendritic spine heads of D1- and D2-MSNs

We next determined whether heroin cue- and extinction-induced MMP-2,9 gelatinolytic activity was localized around dendritic spine heads relative to the dendritic shaft. D1- and D2-MSNs from the saline, extinguished, and 15 min cued heroin seeking rats were analyzed for dendritic spine morphology and specific MMP-2,9 localization at the spine head versus shaft dendritic subcompartments. Figure 3A–C shows the workflow involved in isolating gelatinolytic puncta adjacent to dendritic spine heads versus shafts. Fifteen min after presenting heroin cues D1-MSN spine head diameter increased compared to yoked-saline and heroin-extinguished rats (Figure 3D), while spine density was not different between treatment groups (Figure S3A). MMP-2,9 activity around D1-MSN dendritic spine heads and shafts was also increased by heroin cues, but proportionally more gelatinolytic activity was increased proximal to spine heads relative to shafts, as indicated by an elevated spine head:shaft ratio (Figure 3E).

There was no difference in D2-MSN spine head diameter or density between any of the treatment groups (Figure 3F, S3A). MMP-2,9 activity was increased in heroin-extinguished rats compared to yoked-saline and heroin cued rats, and the increase was proportionally greater around spine heads than dendritic shafts (Figure 3G).

MMP-9 activity increased around D1-MSNs, and MMP-2 activity around D2-MSNs

In vivo zymography cannot distinguish changes in activity between MMP-2 versus MMP-9 (22). To determine whether MMP-2 or MMP-9 was mediating increase gelatinolytic activity, we utilized pharmacological inhibitors with ~20-fold selectivity (37, 38) for each respective gelatinase (Figure 4A). Vehicle (1% DMSO) and inhibitor (0.1 nmol) were microinjected into opposite NAcore hemispheres 15 min prior to starting a 15 min cue-induced reinstatement session for D1-Cre rats. For D2-Cre rats, inhibitor or vehicle was microinjected 30 min prior to sacrifice and 24 hrs after the last extinction session. FITC quenched gelatin substrate was microinjected into NAcore (Figure S4A) 15 min prior to sacrifice in all groups. At low magnification, there were no differences in fluorescence between MMP inhibitor and vehicle in the NAcore of either D1- or D2-Cre rats (Figure S4B). Analysis for cell subtype specific effects revealed that MMP-9i, but not MMP-2i, reduced gelatinolytic activity around D1-MSN dendrites compared to vehicle during cued heroin seeking (Figure 4B), consistent with the involvement of MMP-9 activity in transient forms of synaptic plasticity (39). For D2 MSNs, MMP-2i, but not MMP-9i, reduced gelatinolytic activity compared to vehicle following extinction training (Figure 4C), consistent with the constitutive nature of MMP-2 activity at excitatory synapses (40).

Heroin cues increased astroglia association with synaptic MMP-2,9 activity

Astroglia undergo morphological adaptations in the NAcore after 2–3 weeks of heroin withdrawal and after cued seeking (36), and we next determined if these morphological

adaptations were associated with changes in MMP-2,9 activity. Astroglia in the NAcore of male and female D1/D2-Cre wildtype rats were transfected with a membrane-bound fluorescent reporter (AAV5-GFAP-hM3dq-mCherry) and the proximity of astroglial cell surfaces to the synaptic biomarker protein, Synapsin I, was quantified. Rats were yoked-saline controls or trained to self-administer heroin, extinguished, and some rats were reinstated using heroin-paired cues for 15 min (Figure 5A, S5A,B). Tissue was obtained either 24 hr after the last extinction session or after 15 min of cued reinstatement. Total MMP-2,9 gelatinolytic puncta and Synapsin I were normalized to the volume of each respective mCherry-labeled astrocyte (Figure 5B–E). Co-registration of the astroglial membrane with Synapsin I was reduced after heroin extinction relative to yoked-saline rats, and synaptic proximity was restored after 15 min of cue-induced heroin seeking (Figure 5C). There was no difference in total Synapsin I across groups, indicating changes in astrocyte proximity and not number of synaptic contacts mediated the group differences in co-registration of Synapsin I and astroglial surfaces (Figure S5C). Co-registration between astroglia and MMP gelatinolytic puncta was reduced following heroin extinction training and was partially restored by heroin cues (Figure 5D). Triple co-registration between MMP-2,9 and both Synapsin I and astroglial surfaces reduced after extinction training, but cue-induced heroin seeking increased MMP puncta accumulation within regions positive for Synapsin I and the astroglia mCherry signal (Figure 5E). Quantification of total overall MMP-2,9 fluorescence showed no difference between treatment groups (Figure S5D) (17), and no sex differences were apparent for MMP-Synapsin I-astroglia colocalization (Figure S5E,F). These data indicate that MMP-2,9 activity was not associated with the constitutive retraction of astroglial processes from NAcore synapses after extinction from heroin use, but was engaged in parallel with the re-association of astroglial processes with synapses produced by 15 min of cue-induced reinstatement.

TIMP-1,2 inhibition potentiates cue-induced heroin seeking

TIMP-1 and −2 are endogenous inhibitors of MMP-2,9, with TIMP-1 having greater affinity for MMP-9 and TIMP-2 greater affinity for MMP-2 (41–43). We next determined if TIMP-1 or −2 inhibition of MMP-2,9 contributed to reinstated heroin seeking. In a pilot experiment, microinjection of neither antibody alone into the NAcore altered cue-induced heroin seeking (Figure S6A). Accordingly, we combined the TIMP-1 and TIMP-2 antibodies for subsequent experiments. D1/D2-Cre wildtype rats were trained to self-administer heroin, extinguished and pre-treated with a combination of TIMP-1 and −2 antibodies into NAcore 15 min prior to initiating a 30 min extinction session (refraining) (Figure 6A,B). TIMP-1,2 antibody treatment did not alter lever pressing during refraining compared to extinction baseline (Figure 6C), nor did TIMP-1,2 antibody treatment alter MMP-2,9 activity during extinction training compared to control rats, indicating that minimal TIMP-1,2 tone was present in heroin extinguished rats (Figure 6D; Figure S6B). However, using a within-subject crossover design to pretreat rats with either IgG control or combined TIMP-1,2 neutralizing antibodies in NAcore 15 min prior to a 30 min cued heroin reinstatement session (Figure 6A), TIMP-1,2 antibody augmented cued heroin seeking (Figure 6E), which was driven largely by an increase in active lever pressing during the first 15 min of the reinstatement session (Figure 6E inset). Increased cued heroin seeking was associated with elevated MMP-2,9 activity in TIMP-1,2 antibody-treated animals compared to IgG controls

(Figure 6F; Figure S6C), indicating that TIMP-1,2 tone was increased by heroin-paired cues. Combined TIMP-1,2 antibody treatment did not affect locomotor activity (Figure S6D), and the microinjection cannula tips for all rats were bilaterally localized to the NAcore (Figure S6E).

Selective elevation in TIMP-1,2 in D1-MSNs during extinction and D2-MSNs during reinstated heroin seeking

The potentiation of cued heroin seeking indicated that there was a cue-induced increase in TIMP-1,2 inhibition of MMP-2,9 that dampened heroin seeking, and posed the possibility that, akin to MMP-2 versus MMP-9, TIMP-1 or −2 may show differential cell-specific expression around D1- and D2-MSNs. To determine if TIMP-1 and - 2 exhibited cell-type specific expression, mCherry transfected D1- and D2-Cre rats underwent yoked-saline or heroin self-administration and extinction, followed by 15 min of cue-induced reinstatement (Figure S7A,B). D1- and D2-Cre rats demonstrated equivalent behavior (Figure S7A,B). Brain sections from NAcore of yoked saline, extinguished and heroin seeking rats were stained for TIMP-1 and −2 immunoreactivity (Figure 6G–J). TIMP-1 immunoreactivity was greater than TIMP-2 in yoked-saline animals around both MSN subtypes (compare SAL groups in figure 6G,H with figure 6I,J). Extinction training was associated with increased TIMP-2 selectively around D1-MSNs (Figure 6I). In contrast, cued seeking was associated with elevated TIMP-1 and −2 around D2-MSNs (Figure 6H,J), with no change in either TIMP-1 or −2 around D1-MSNs compared to yoked-saline (Figure 6G,I). Importantly, there was no difference in total TIMP-1 and −2 expression normalized to the volume of the image series across SAL, EXT, and RST 15’ groups between D1 and D2 MSN cell-types (Figure S7E,F), indicating that the group differences in TIMP immunoreactivity resulted from differences in cell specific localization, not differences in overall TIMP levels.

Discussion

We demonstrated that cue-induced heroin seeking and extinguished refraining are associated with activation of different MMPs (−2 or −9) around different NAcore cell types (D1-, D2-MSNs and astroglia). Enduring MMP-2 proteolytic activity was increased selectively around D2-MSNs by extinction training. However, when heroin-paired cues were available, MMP-2 activity was reduced around D2-MSNs, and MMP-9 activity was elevated around D1-MSNs. The cue-induced changes in MMP activity were transient, and once cue-responding was extinguished (after 120 min of cue availability without receiving heroin reward), the extinguished state of elevated MMP-2 activity around D2-MSNs and baseline MMP-9 activity around D1-MSNs was restored. The transient inhibition of MMP-2 activity around D2-MSNs was likely mediated by a cell-type selective increases in TIMP-1 and −2, and when TIMP-1,2 inhibitory activity was blocked cue-induced heroin seeking increased, indicating that cue-induced reductions in MMP-2,9 activity negatively regulate heroin seeking. Together, these data show that MMP-2,9 activity and corresponding signaling to different compartments of NAcore tetrapartite synapses is regulated by behavioral states related to opioid addiction and is consequential in the capacity of rats to refrain from or seek heroin after a period of drug withdrawal. Figure S8 summarizes the differential actions of MMP-2,9 and TIMP1,2 on different cell types during different behavioral states.

Tetrapartite synapses and cue-induced heroin seeking

Tetrapartite synapses in the NAcore undergo transient plasticity in response to drug-paired cues that induce drug seeking (13, 44). Supporting a role for MMP-9 activation in tetrapartite synaptic plasticity, the increased gelatinase activity around D1- MSNs during heroin seeking was localized to a greater extent around dendritic spine heads than the dendritic shaft. Cue-induced MMP-9 activation promotes drug seeking by cleaving ECM proteins (41), creating ligands that stimulate β3-integrin receptors and signal spine head expansion through phosphorylating focal adhesion kinase (24). Like the increase in MMP-9 activity, the MMP-dependent postsynaptic signaling and potentiation is transient, selective for D1-MSNs and necessary for cues to induce drug seeking (6, 28, 45). However, not all drug use-associated changes in tetrapartite synaptic plasticity facilitate drug seeking. Notably, heroin cues induce transient re-association of astroglial processes with NAcore synapses that limits cued heroin seeking (16). The fact that we found cued astroglial proximity to synapses was associated with elevated MMP activity indicates that this astroglial morphological adaptation likely corresponds to MMP-9 activation at D1-MSN synapses since cues elevate MMP-9 activity selectively at D1-MSNs, while reducing MMP-2 activity at D2-MSNs.

Tetrapartite synapses and refraining from drug seeking

Extinction from heroin seeking produced an enduring elevation in MMP-2 activity selectively around D2-MSNs. It is tempting to consider that this cell-type specific activity is associated with tetrapartite neuroadaptations underpinning refraining from heroin seeking in an extinguished heroin-associated context. Supporting this possibility, MMP-2 activity was reduced when heroin-paired cues were presented to motivate rats to seek drug in an extinguished context. Also, the association of MMP-2 activity with D2-MSNs is consistent with the well-established role of D2-MSN activation at inhibiting motivated behaviors (9, 10, 46). Also, we found that the time course of MMP-2 inactivation paralleled the motivation to seek heroin. Thus, MMP-2 activity was reduced after 15 min of active cued seeking and elevated during extinguished responding after 120 min of cue-induced reinstatement. Finally, TIMP-1 and −2 immunoreactivity was elevated selectively around D2-MSNs after 15 min of cued heroin seeking, supporting the hypothesis that the cue-induced reduction in MMP-2 arises from increased TIMP-1,2 inhibition of enzyme activity. Contrasting a role for reduced MMP-2 around D2-MSNs in facilitating cued-reinstatement, when TIMP-1,2 inhibition induced by cues was blocked by antibody neutralization, heroin seeking was promoted, indicating that the TIMP-dependent inhibition of MMP-2 may function in a compensatory manner to reduce cued heroin seeking. However, it is also possible that the elevation in heroin seeking seen after inhibiting TIMP-1,2 could be mediated by removing inhibition on D1-MSN-associated MMP-9, which would reduce drug refraining and elevate seeking.

Methodological considerations for *in vivo* zymography

In vivo zymography fluorescence increases linearly over time (17), and our studies capture a “snapshot” in time, making it difficult to discern directionality in the role of elevated MMP-2,9 and TIMP-1,2. Nonetheless, the cell-type specific observations display a unique distribution pattern not represented by overall gelatinase activity or TIMP-1,2

immunoreactivity in NAcore (Figure S2D, S7E,F). Similarly, MMP-2,9 activity measured across treatment groups used for quantifying MMP-2,9 activity associated with astrocytes and the synaptic marker Synapsin I (Figure S5C,D). These findings support the notion that distinct cell group specific ECM signaling was differentially associated with heroin seeking and refraining regardless of overall MMP activity and TIMP-1,2 expression in NAcore. However, analysis in a single window of time leaves open questions regarding how MMP activity in each cell type may be correlated with other tetrapartite synaptic adaptations produced during cued heroin seeking.

Another question in these studies is how MMPs display cell-type and subcompartment specific activity despite being released by both MSNs and astrocytes. Signaling process, possibly nitrosylation or proteolytic cleavage, may be responsible for selective release and activation of MMPs by a cell-type. For example, MMP-2 and MMP-9 are differentially expressed in T-lymphocytes depending on which ligand binds to integrin α4β1 molecule (47). Further investigation is warranted to fully disentangle this level of complexity to translate focal MMP physiology into a drug seeking phenotype.

Conclusion

We discovered that MMP-induced signaling in the ECM is differentially organized around distinct cell populations to selectively regulate different addiction-associated behaviors in an animal model of OUD. The changes in MMP catalytic signaling involved not just classic neuronal synaptic plasticity around D1- and D2-MSNs, but also affected astroglia. These findings highlight that in order to accurately develop successful therapeutic interventions for opioid mediated synaptic pathologies, it is necessary to understand not only classic pre- and postsynaptic adaptations, but also how these adaptations interface with parallel plasticity in the other two tetrapartite synaptic compartments, astroglia proximal to the synapse and ECM signaling by MMPs.

Supplementary Material

Refer to Web version on PubMed Central for supplementary material.

Acknowledgements

We thank Eric Dereschewitz, Constanza Garcia-Keller, and Brittany Kuhn for advice and technical support. This work was supported by the National Institute of Health DA046143 (V.C.C), DA044782 (A.K.), DA046522 (A-C.B.), DA040004 (M.D.S.), DA003906 (P.W.K), and DA12513 (P.W.K).

References

1. Strang J, Volkow ND, Degenhardt L, Hickman M, Johnson K, Koob GF, et al. (2020): Opioid use disorder. Nature Reviews Disease Primers. 6:3.
2. Kruyer A, Chioma VC, Kalivas PW (2020): The Opioid-Addicted Tetrapartite Synapse. Biological Psychiatry. 87:34–43. [PubMed: 31378302]
3. Hearing M, Graziane N, Dong Y, Thomas MJ (2018): Opioid and Psychostimulant Plasticity: Targeting Overlap in Nucleus Accumbens Glutamate Signaling. Trends Pharmacol Sci. 39:276–294. [PubMed: 29338873]

4. Floresco SB (2015): The Nucleus Accumbens: An Interface Between Cognition, Emotion, and Action. Annual Review of Psychology. 66:25–52.
5. Graziane NM, Sun S, Wright WJ, Jang D, Liu Z, Huang YH, et al. (2016): Opposing mechanisms mediate morphine- and cocaine-induced generation of silent synapses. Nat Neurosci. 19:915–925. [PubMed: 27239940]
6. Shen H, Moussawi K, Zhou W, Toda S, Kalivas PW (2011): Heroin relapse requires long-term potentiation-like plasticity mediated by NMDA2b-containing receptors. Proceedings of the National Academy of Sciences of the United States of America. 108:19407–19412. [PubMed: 22084102]
7. Shen HW, Scofield MD, Boger H, Hensley M, Kalivas PW (2014): Synaptic glutamate spillover due to impaired glutamate uptake mediates heroin relapse. J Neurosci. 34:5649–5657. [PubMed: 24741055]
8. Roberts-Wolfe D, Bobadilla AC, Heinsbroek JA, Neuhofer D, Kalivas PW (2018): Drug Refraining and Seeking Potentiate Synapses on Distinct Populations of Accumbens Medium Spiny Neurons. J Neurosci. 38:7100–7107. [PubMed: 29976626]
9. Heinsbroek JA, Neuhofer DN, Griffin WC 3rd, Siegel GS, Bobadilla AC, Kupchik YM, et al. (2017): Loss of Plasticity in the D2-Accumbens Pallidal Pathway Promotes Cocaine Seeking. J Neurosci. 37:757–767. [PubMed: 28123013]
10. Lobo MK, Nestler EJ (2011): The striatal balancing act in drug addiction: distinct roles of direct and indirect pathway medium spiny neurons. Frontiers in neuroanatomy. 5:41. [PubMed: 21811439]
11. Terrier J, Luscher C, Pascoli V (2016): Cell-Type Specific Insertion of GluA2-Lacking AMPARs with Cocaine Exposure Leading to Sensitization, Cue-Induced Seeking, and Incubation of Craving. Neuropsychopharmacology. 41:1779–1789. [PubMed: 26585289]
12. Bobadilla AC, Heinsbroek JA, Gipson CD, Griffin WC, Fowler CD, Kenny PJ, et al. (2017): Corticostriatal plasticity, neuronal ensembles, and regulation of drug-seeking behavior. Prog Brain Res. 235:93–112. [PubMed: 29054293]
13. Mulholland PJ, Chandler LJ, Kalivas PW (2016): Signals from the Fourth Dimension Regulate Drug Relapse. Trends Neurosci. 39:472–485. [PubMed: 27173064]
14. Wang J, Li K-L, Beroun A, Ishikawa M, Huang X, Wang YQ, et al. (2020): Cocaine triggers astrocyte-mediated synaptogenesis. Biological Psychiatry. in press.
15. Scofield MD, Li H, Siemsen BM, Healey KL, Tran PK, Woronoff N, et al. (2016): Cocaine Self-Administration and Extinction Leads to Reduced Glial Fibrillary Acidic Protein Expression and Morphometric Features of Astrocytes in the Nucleus Accumbens Core. Biol Psychiatry. 80:207–215. [PubMed: 26946381]
16. Kruyer A, Scofield MD, Wood D, Reissner KJ, Kalivas PW (2019): Heroin Cue-Evoked Astrocytic Structural Plasticity at Nucleus Accumbens Synapses Inhibits Heroin Seeking. Biol Psychiatry. 86:811–819. [PubMed: 31495448]
17. Smith AC, Kupchik YM, Scofield MD, Gipson CD, Wiggins A, Thomas CA, et al. (2014): Synaptic plasticity mediating cocaine relapse requires matrix metalloproteinases. Nat Neurosci. 17:1655–1657. [PubMed: 25326689]
18. Testen A, Sepulveda-Orengo MT, Gaines CH, Reissner KJ (2018): Region-Specific Reductions in Morphometric Properties and Synaptic Colocalization of Astrocytes Following Cocaine Self-Administration and Extinction. Frontiers in cellular neuroscience. 12:246. [PubMed: 30147645]
19. Spencer S, Garcia-Keller C, Roberts-Wolfe D, Heinsbroek JA, Mulvaney M, Sorrell A, et al. (2017): Cocaine Use Reverses Striatal Plasticity Produced During Cocaine Seeking. Biol Psychiatry. 81:616–624. [PubMed: 27837917]
20. Tsilibary E, Tzinia A, Radenovic L, Stamenkovic V, Lebitko T, Mucha M, et al. (2014): Neural ECM proteases in learning and synaptic plasticity. Prog Brain Res. 214:135–157. [PubMed: 25410356]
21. Soleman S, Filippov MA, Dityatev A, Fawcett JW (2013): Targeting the neural extracellular matrix in neurological disorders. Neuroscience. 253:194–213. [PubMed: 24012743]
22. Huntley GW (2012): Synaptic circuit remodelling by matrix metalloproteinases in health and disease. Nat Rev Neurosci. 13:743–757. [PubMed: 23047773]

23. Szepesi Z, Hosy E, Ruszczycki B, Bijata M, Pyskaty M, Bikbaev A, et al. (2014): Synaptically released matrix metalloproteinase activity in control of structural plasticity and the cell surface distribution of GluA1-AMPA receptors. PLoS One. 9:e98274. [PubMed: 24853857]
24. Garcia-Keller C, Neuhofer D, Bobadilla AC, Spencer S, Chioma VC, Monforton C, et al. (2019): Extracellular Matrix Signaling Through beta3 Integrin Mediates Cocaine Cue-Induced Transient Synaptic Plasticity and Relapse. Biol Psychiatry. 86:377–387. [PubMed: 31126696]
25. Smith AC, Scofield MD, Heinsbroek JA, Gipson CD, Neuhofer D, Roberts-Wolfe DJ, et al. (2017): Accumbens nNOS Interneurons Regulate Cocaine Relapse. J Neurosci. 37:742–756. [PubMed: 28123012]
26. Brown TE, Forquer MR, Cocking DL, Jansen HT, Harding JW, Sorg BA (2007): Role of matrix metalloproteinases in the acquisition and reconsolidation of cocaine-induced conditioned place preference. Learn Mem. 14:214–223. [PubMed: 17353546]
27. Samochowiec A, Grzywacz A, Kaczmarek L, Bienkowski P, Samochowiec J, Mierzejewski P, et al. (2010): Functional polymorphism of matrix metalloproteinase-9 (MMP-9) gene in alcohol dependence: family and case control study. Brain Research. 1327:103–106. [PubMed: 20197064]
28. Garcia-Keller C, Scofield M, Neuhofer D, Varanaxi S, Anderson E, Richie CT, et al. (2020): Relapse-associated transient synaptic plasticity requires integrin-mediated activation of focal adhesion kinase and cofilin. Journal of Neuroscience. in press.
29. Reikvam H, Hatfield KJ, Øyan AM, Kalland KH, Kittang AO, Bruserud Ø (2010): Primary human acute myelogenous leukemia cells release matrix metalloproteases and their inhibitors: release profile and pharmacological modulation. European Journal of Haematology. 84:239–251. [PubMed: 19922462]
30. Lu D, Liao Y, Zhu S-H, Chen Q-C, Xie D-M, Liao J-J, et al. (2019): Bone-derived Nestin-positive mesenchymal stem cells improve cardiac function via recruiting cardiac endothelial cells after myocardial infarction. Stem Cell Res Ther. 10:127–127. [PubMed: 31029167]
31. Rossello A, Nuti E, Orlandini E, Carelli P, Rapposelli S, Macchia M, et al. (2004): New N-arylsulfonyl-N-alkoxyaminoacetohydroxamic acids as selective inhibitors of gelatinase A (MMP-2). Bioorganic & Medicinal Chemistry. 12:2441–2450. [PubMed: 15080939]
32. Levin JI, Chen J, Du M, Hogan M, Kincaid S, Nelson FC, et al. (2001): The discovery of anthranilic acid-Based MMP inhibitors. Part 2: SAR of the 5-position and P11 groups. Bioorganic & Medicinal Chemistry Letters. 11:2189–2192. [PubMed: 11514167]
33. Zhou W, Kalivas PW (2008): N-acetylcysteine reduces extinction responding and induces enduring reductions in cue- and heroin-induced drug-seeking. Biological psychiatry. 63:338–340. [PubMed: 17719565]
34. Shen H, Sesack SR, Toda S, Kalivas PW (2008): Automated quantification of dendritic spine density and spine head diameter in medium spiny neurons of the nucleus accumbens. Brain Structure and Function. 213:149–157. [PubMed: 18535839]
35. Siemsen BM, Giannotti G, McFaddin JA, Scofield MD, McGinty JF (2019): Biphasic effect of abstinence duration following cocaine self-administration on spine morphology and plasticity-related proteins in prelimbic cortical neurons projecting to the nucleus accumbens core. Brain Struct Funct. 224:741–758. [PubMed: 30498893]
36. Kruyer A, Scofield MD, Wood D, Reissner KJ, Kalivas PW (2019): Heroin Cue–Evoked Astrocytic Structural Plasticity at Nucleus Accumbens Synapses Inhibits Heroin Seeking. Biological Psychiatry. 86:811–819. [PubMed: 31495448]
37. Rossello A, Nuti E, Orlandini E, Carelli P, Rapposelli S, Macchia M, et al. (2004): New N-arylsulfonyl-N-alkoxyaminoacetohydroxamic acids as selective inhibitors of gelatinase A (MMP-2). Bioorg Med Chem. 12:2441–2450. [PubMed: 15080939]
38. Levin JI, Chen J, Du M, Hogan M, Kincaid S, Nelson FC, et al. (2001): The discovery of anthranilic acid-based MMP inhibitors. Part 2: SAR of the 5-position and P1(1) groups. Bioorg Med Chem Lett. 11:2189–2192. [PubMed: 11514167]
39. Michaluk P, Kolodziej L, Mioduszewska B, Wilczynski GM, Dzwonek J, Jaworski J, et al. (2007): β-Dystroglycan as a Target for MMP-9, in Response to Enhanced Neuronal Activity. Journal of Biological Chemistry. 282:16036–16041.

40. Verslegers M, Lemmens K, Van Hove I, Moons L (2013): Matrix metalloproteinase-2 and −9 as promising benefactors in development, plasticity and repair of the nervous system. Progress in Neurobiology. 105:60–78. [PubMed: 23567503]

41. Vafadari B, Salamian A, Kaczmarek L (2016): MMP-9 in translation: from molecule to brain physiology, pathology, and therapy. J Neurochem. 139 Suppl 2:91–114.

42. Sánchez-Pozo J, Baker-Williams AJ, Woodford MR, Bullard R, Wei B, Mollapour M, et al. (2018): Extracellular Phosphorylation of TIMP-2 by Secreted c-Src Tyrosine Kinase Controls MMP-2 Activity. iScience. 1:87–96. [PubMed: 30227959]

43. Hu J, Van den Steen PE, Sang QX, Opdenakker G (2007): Matrix metalloproteinase inhibitors as therapy for inflammatory and vascular diseases. Nat Rev Drug Discov. 6:480–498. [PubMed: 17541420]

44. Scofield MD, Heinsbroek JA, Gipson CD, Kupchik YM, Spencer S, Smith AC, et al. (2016): The Nucleus Accumbens: Mechanisms of Addiction across Drug Classes Reflect the Importance of Glutamate Homeostasis. Pharmacol Rev. 68:816–871. [PubMed: 27363441]

45. Gipson CD, Kupchik YM, Shen H, Reissner KJ, Thomas CA, Kalivas PW (2013): Relapse induced by cues predicting cocaine depends on rapid, transient synaptic potentiation. Neuron. 77:867–872. [PubMed: 23473317]

46. Kravitz AV, Tye LD, Kreitzer AC (2012): Distinct roles for direct and indirect pathway striatal neurons in reinforcement. Nat Neurosci. 15:816–818. [PubMed: 22544310]

47. Yakubenko VP, Lobb RR, Plow EF, Ugarova TP (2000): Differential Induction of Gelatinase B (MMP-9) and Gelatinase A (MMP-2) in T Lymphocytes upon α4β1-Mediated Adhesion to VCAM-1 and the CS-1 Peptide of Fibronectin. Experimental Cell Research. 260:73–84. [PubMed: 11010812]

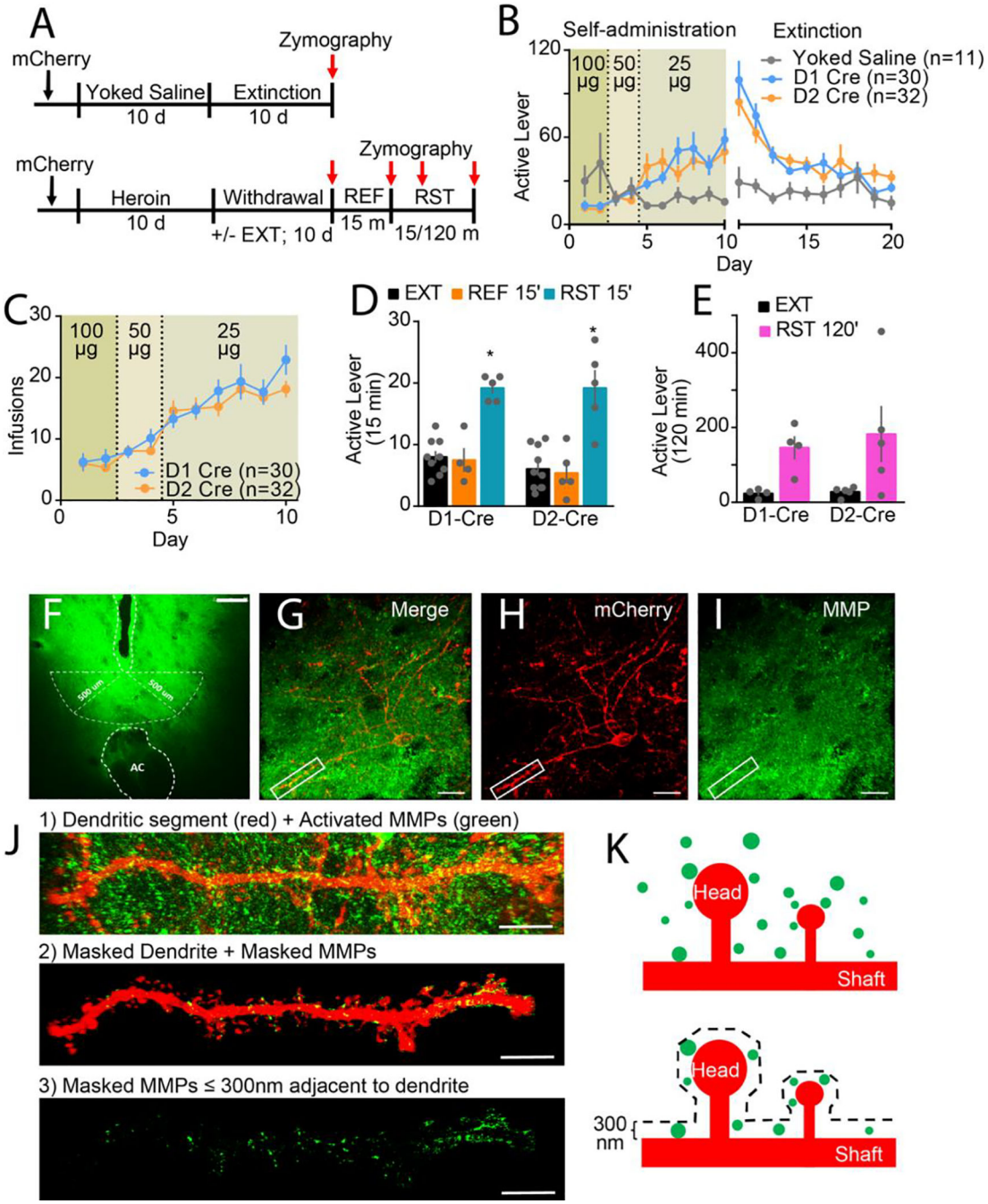

Figure 1. Heroin self-administration, extinction, and behavioral responding in D1- and D2-Cre rats.

A) Experimental timeline outlining heroin self-administration (Self-ad), withdrawal (with or without extinction training [EXT]), refraining (REF) and reinstatement (RST). **B)** Time course of active lever pressing in D1- and D2-Cre rats during heroin self-administration and extinction. The genotypes had similar behavior (2-way ANOVA; genotype $F_{(1,52)}$=0.041; p=0.841; time $F_{(19,988)}$=18.94; p<0.001; interaction $F_{(19,988)}$=1.03; p=0.428), and heroin emitted more lever presses than yoked saline (2-way ANOVA; treatment group $F_{(2,60)}$=3.94,

p=0.025; time $F_{(19,1140)}$=7.49, p<0.001; interaction $F_{(38,1140)}$=2.62, p<0.001). **C)** No genotypic differences in escalation of heroin infusions (2-way ANOVA; genotype $F_{(1,52)}$=1.59; p=0.213; effect of time $F_{(9,468)}$=29.70; p<0.001; interaction $F_{(9,468)}$=0.90; p=0.527). **D)** No genotypic differences in active lever presses for refraining during a 15 min extinction session or reinstatement (2-way ANOVA; interaction $F_{(5,22)}$=10.02; p<0.001; D1 cre: EXT/RST $F_{(5,22)}$=6.21; p<0.001; D2 cre: EXT/RST $F_{(5,22)}$=6.56; p<0.001). **E)** No genotypic differences in cue-induced reinstatement of heroin-seeking active lever presses over 120 mins (2-way ANOVA; genotype $F_{(1,7)}$=0.18; p=0.686; EXT/RST $F_{(1,7)}$=11.07; p=0.013; interaction $F_{(1,7)}$=0.15; p=0.709). Each dot in bar represents an animal. Data are shown as mean ± SEM. *p<0.05 comparing EXT and EXT 15' to RST 15' or RST 120' using Sidak post hoc test. **F)** Representative micrograph of *in vivo* zymography assay in NAcore, 10x. White dotted lines outline the injection track and anterior commissure (AC). Higher magnification imaging of accumbens cell types occurred ≤500 μm from the microinjector tip, which is demarcated with white dotted semi-circle. Bar=250 μm. **G)** Merge of **H)** mCherry-labeled MSN (red) surrounded by **I)** MMP activity (green) in NAcore, 63x. White box in **G-I** indicates dendritic segment and MMP activity imaged for Imaris processing in panel e. Bar=20 μm. **J)** High resolution representative micrographs of Imaris 3D rendering workflow for MMP quantification around MSN dendrite, 63x. *1)* Raw confocal image of dendritic segment (red) and activated MMP gelatinolytic puncta (green). *2)* Isolated dendrite used to mask out MMP puncta not within 300 nm of dendritic surface. *3)* Only masked MMPs ≤ 300 nm adjacent to dendrite shown and quantified. **K)** Model of MMP gelatinolytic puncta (green) surrounding mCherry-labeled MSN (red) with dendritic spine heads and shaft subcompartments indicated. MMP gelatinolytic puncta within 300 nm of dendrite surface were isolated and normalized to volume around dendrite in which they occupy to calculate % MMP activity around dendritic segment.

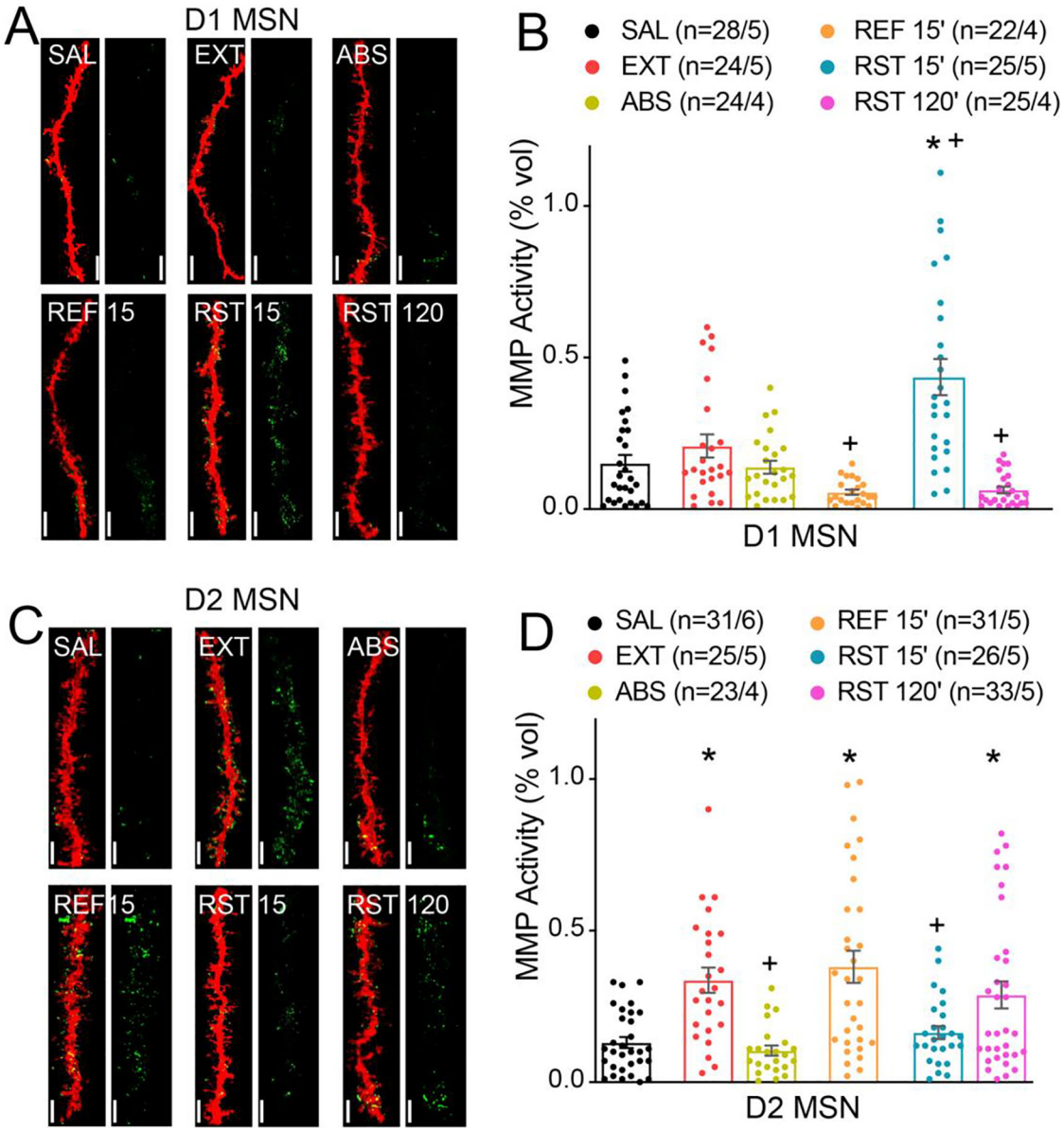

Figure 2. MMP-2 and MMP-9 activity localize differentially around D1- and D2-MSNs during heroin seeking and extinction.

A) Representative images of 3D reconstruction of mCherry-labeled D1 MSN dendritic segments (red) and MMP gelatinolytic puncta (green) localized within 300 nm of dendrite surface for each group yoked saline (SAL), withdrawn with extinction (EXT), withdrawn without extinction (ABS), 15 min in the extinguished environment (REF 15'), RST 15' and RST 120'. Bar=7 μm. **B)** Transient heroin seeking induces significant increase in active MMP puncta localization around D1 MSNs (Nested ANOVA; $F_{(4,17)}$=6.41; p=0.003). **c)** Representative images of 3D reconstruction of mCherry-labeled D2 MSN dendritic segments. Bar=7 μm. **d)** Extinction training induced increase in active MMP puncta localization around D2 MSNs (Nested ANOVA; $F_{(5, 24)}$=6.50; p<0.001). Data are shown as mean ± SEM. N represents number of neurons quantified over number of in each condition. *p<0.05 compared to SAL, +p<0.05 compared to EXT, using Sidak post hoc test.

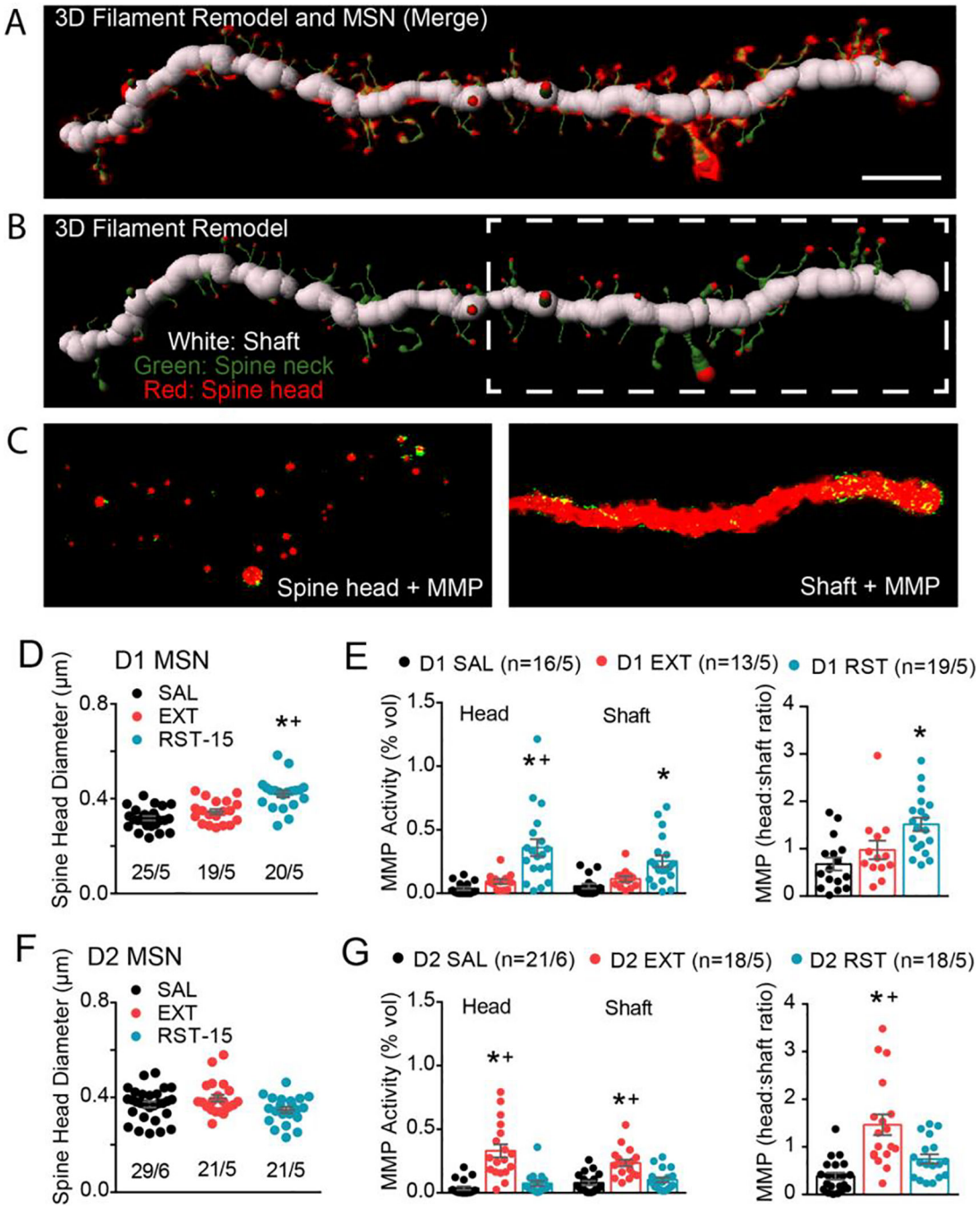

Figure 3. Quantitative isolation of MMP-2,9 activity around the dendritic spine heads versus dentrite shaft of D1- and D2-MSNs.

A) Merge of filament 3D remodel and isolated dendritic segment from Figure 2e. **B)** The 3D filament remodel recapitulates the dendritic shaft (white), spine neck (green), and spine head (red) (middle panel). White dashed box highlights region of dendrite conveyed in bottom panel. **C)** The 3D space-filling model of spine heads or shaft was used to mask MMP-2/9 puncta not associated to either the spine head (left panel) or dendrite shaft (right panel) compartments in order to calculate 1) spine head-specific and 2) shaft-specific

MMP puncta localization. Scale bar=5μm. **D)** D1 MSNs exhibit potentiated spine head diameter during transient heroin seeking (nested 1-way ANOVA; $F_{(2, 12)}$=8.28; p=0.006). **E)** MMP gelatinolytic puncta was increased in both spine head and shaft subcompartments of D1 dendritic segments during transient heroin seeking (nested 1-way ANOVA; spine head $F_{(2, 12)}$=11.80; p=0.002; shaft $F_{(2, 12)}$=7.77; p=0.007). Spine head:Shaft MMP ratio revealed increased spine head-specific MMP gelatinolytic puncta around D1-MSNs during cue-induced RST (nested 1-way ANOVA, $F_{(2, 12)}$=7.49; p=0.008). **c)** No difference D2-MSN spine head diameter across groups (nested ANOVA; $F_{(2, 13)}$=2.455; p=0.1246). **F)** MMP gelatinolytic puncta was increased in both spine head and shaft subcompartments of D2-MSN dendritic segments under extinguished conditions (nested 1-way ANOVA; spine head $F_{(2, 53)}$=25.08; p<0.001; shaft $F_{(2, 13)}$=11.69; p=0.001). **G)** Spine head:Shaft MMP ratio revealed increased spine head-specific MMP gelatinolytic puncta around D2-MSNs following extinction (nested 1-way ANOVA; $F_{(2, 54)}$=15.66; p<0.001). Data are shown as mean ± SEM. N represents number of neurons quantified over number of animals in each condition. *p<0.05 comparing RST or EXT to SAL, $^{+}$p<0.05 comparing RST to EXT using a Sidak post hoc test.

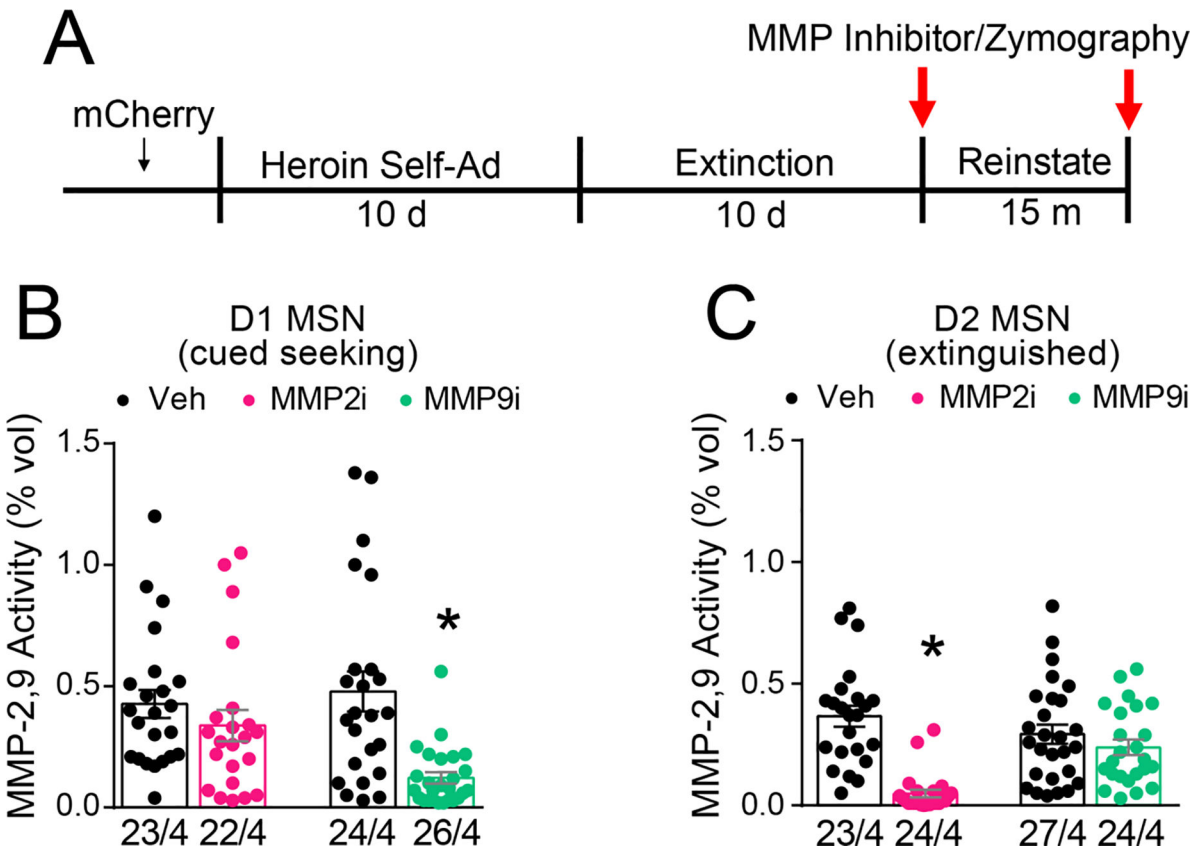

Figure 4. MMP-9 activity increases around D1-MSNs, and MMP-2 around D2-MSNs.

A) Experimental timeline outlining heroin self-administration, extinction, and reinstatement. **B)** Transient MMP gelatinolytic activity around D1 MSNs during cued-heroin seeking was MMP-9-dependent (Nested t-test; Veh/MMP9i, $F_{(1,48)}=18.52$, $p<0.001$; Veh/MMP2i, $F_{(1,6)}=0.68$, $p=0.450$). **C)** Constitutive MMP gelatinolytic activity around D2 MSNs following extinction was MMP-2-dependent (Nested t-test; Veh/MMP2i, $F_{(1,45)}=49.17$, $p<0.001$; Veh/MMP9i; $F_{(1,6)}=0.5387$, $p=0.491$). Data are shown as mean ± SEM. N represents number of neurons quantified over number of animals in each condition. *p< 0.05, compared to vehicle

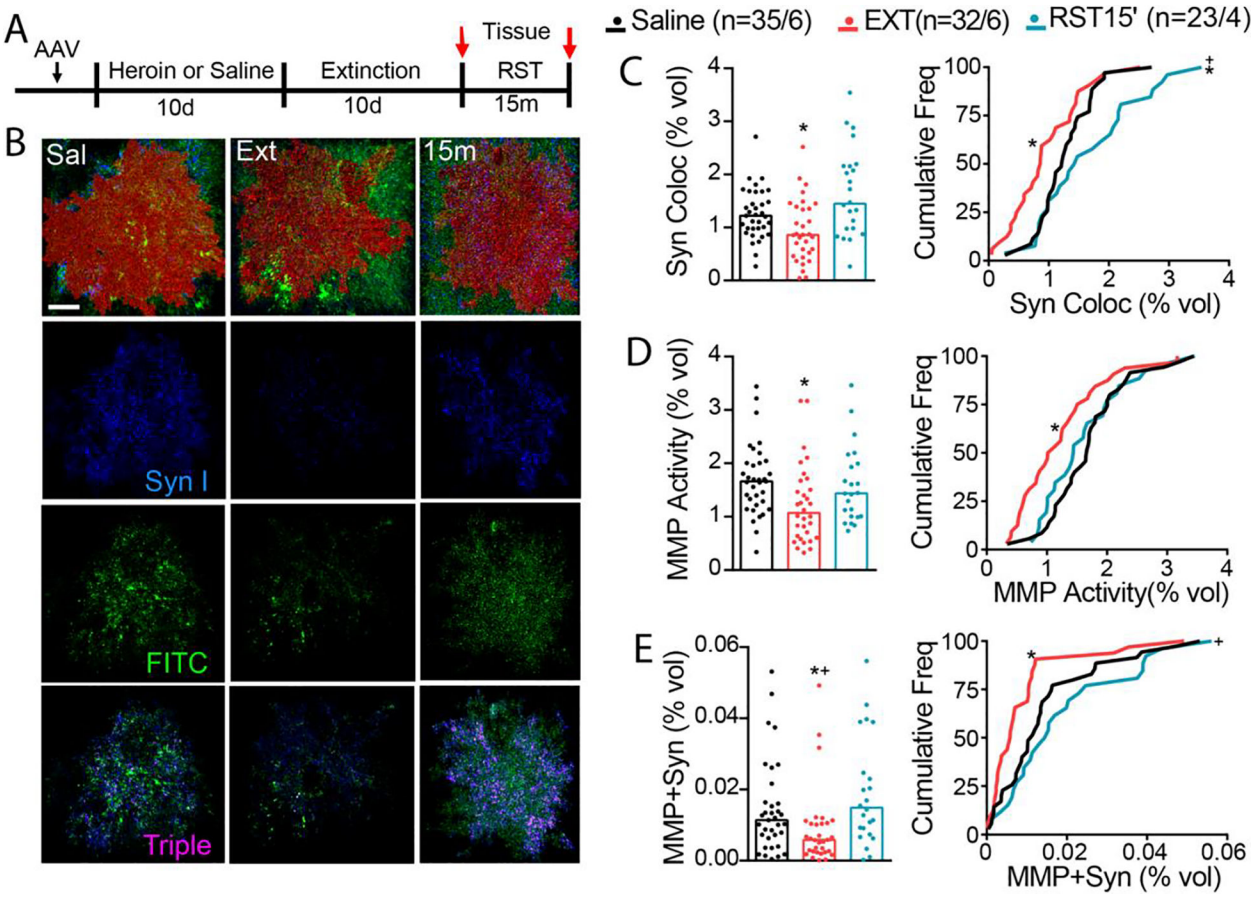

Figure 5. Heroin cues increase astroglia association with synaptic MMP-2,9 activity.

A) Experimental timeline outlining heroin self-administration, extinction, and reinstatement. Rats were trained to self-administer heroin and were subsequently extinguished to the cues associated with heroin infusions. **B)** Imaris quantification workflow for MMP-Synapsin I colocalization. Representative micrographs of digitized 3D model of mCherry-labeled astrocyte (red) for each treatment group (Sal, Ext, and RST 15 m). **C)** Synaptic contact between astrocyte membrane and presynaptic marker synapsin I was reduced after heroin extinction, while cued heroin seeking transiently restored peripheral astroglial processes to synapse (left panel shows raw data points, Kruskal-Wallis=13.32, p=0.001; right panel shows frequency plots, Kolmogorov-Smirnov=0.393, p=0.022). **D)** MMP activity co-registered with astrocyte membrane was decreased after heroin extinction (left panel shows raw data points, Kruskal-Wallis=10.06, p=0.007; right panel shows frequency plots, Kolmogorov-Smirnov=0.386, p=0.028). **E)** MMP gelatinolytic puncta and synapsin co-registry was reduced under extinguished conditions, while transiently increased during cue-induced heroin seeking (left panel shows raw data points, Kruskal-Wallis=12.80, p=0.002; right panel shows frequency plots, Kolmogorov-Smirnov=0.399, p=0.019 for SAL vs EXT, Kolmogorov-Smirnov=0.483, p=0.005 for EXT vs RST). N represents number of cells quantified over number of animals in each condition. Data are shown as median. *p<0.05 compared to SAL, $^{+}$p<0.05 compared to RST using Dunn post hoc test.

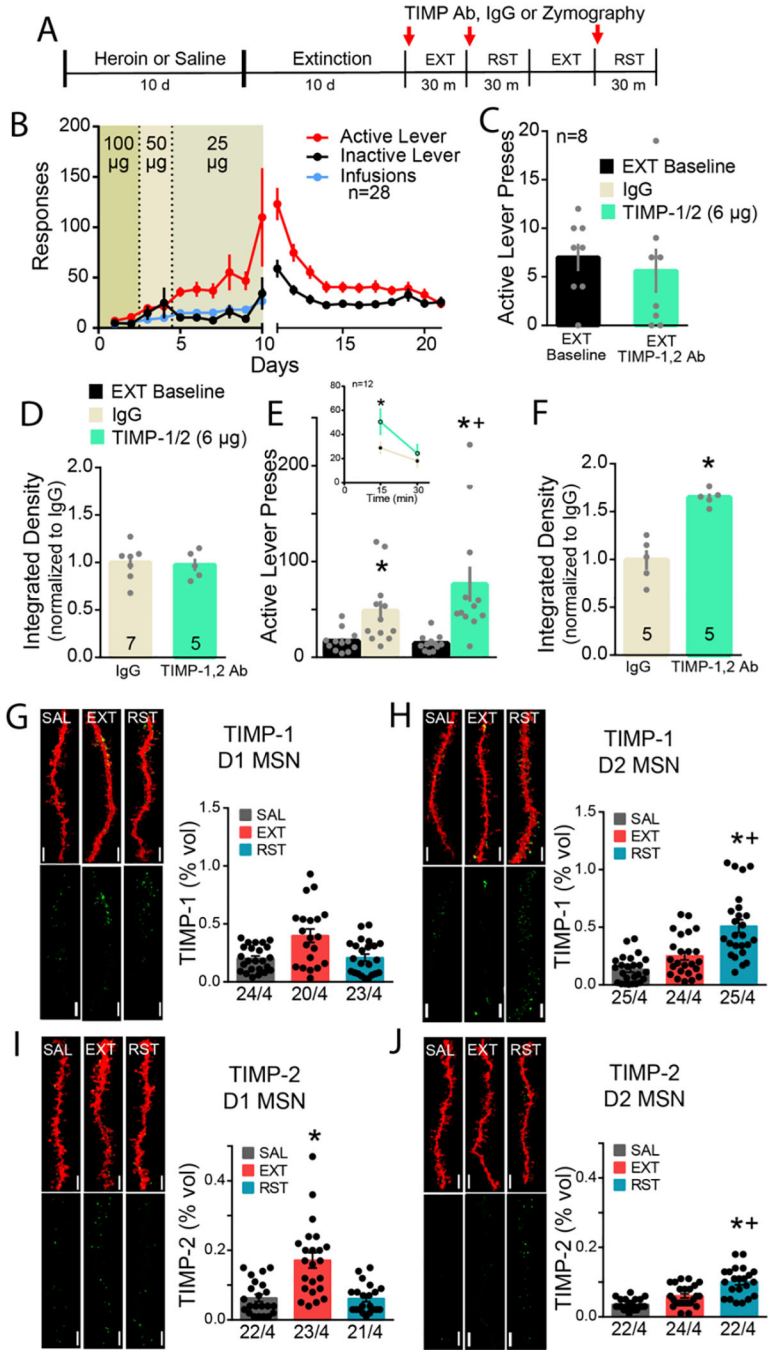

Figure 6. TIMP-1,2 inhibition potentiates cue-induced heroin seeking via cell specific TIMP-1,2 expression around D1 and D2 MSNs.

A) Experimental timeline outlining heroin self-administration, extinction, and reinstatement and TIMP inhibitor cross-over design. **B)** Rats were trained to self-administer heroin and responding to the heroin-paired cues was subsequently extinguished. **C)** No difference in refraining behavior with TIMP-1,2 antibody pre-treatment in NAcore compared to extinction baseline (Paired t-test; $t_{(7)}$=0.83; p=0.434). **D)** No difference in MMP-2,9 activity, quantified as integrated density, in refraining controls compared to TIMP-1,2 antibody-treated animals

(Unpaired t-test; $t_{(10)}$=0.24; p=0.815). **E)** Reinstated animals (t=30 min) received IgG or TIMP-1,2 antibodies microinjected in NAcore in randomized crossover design. Combined TIMP-1,2 inhibition potentiated cued heroin seeking compared to IgG (2-way ANOVA; treatment (IgG/TIMP) $F_{(1,11)}$=6.70; p=0.025; EXT/RST $F_{(1,11)}$=11.56; p=0.006; interaction $F_{(1,11)}$=6.65; p=0.026). No difference in inactive lever presses during cue-induced heroin seeking after IgG or TIMP-1,2 antibody microinjection in NAcore (2-way ANOVA; $F_{(1,11)}$=0.33; p=0.573). **Inset:** Time course of reinstatement session revealed enhanced heroin seeking in first 15 min compared to IgG controls (2-way ANOVA; treatment $F_{(1,22)}$=1.75; p=0.200; time $F_{(1,22)}$=28.40; p<0.001; interaction $F_{(1,22)}$=4.94; p=0.037). **F)** Simultaneous TIMP-1,2 inhibition significantly potentiated MMP-2/9 enzymatic activity in NAcore during cue-induced heroin reinstatement (Unpaired t-test; $F_{(4,4)}$=7.94; p=0.001). N in bars indicates number of animals with an average of four-seven NAcore slices/rat. Bar=250 μm. Data are shown as mean ± SEM and integrated density was normalized to control mean. *p<0.05 compared to extinction, $^{+}$p<0.05 compared to IgG using Sidak post hoc test. **G)** Representative images of 3D reconstruction of mCherry-labeled dendritic segments (red) and TIMP-1 or −2 puncta (green) localized within 300 nm of dendrite surface for each group SAL, EXT, and RST 15’ are shown beside each corresponding graph. No difference in TIMP-1 expression around D1 MSNs across groups (Nested 1-way ANOVA; $F_{(2,9)}$=1.32; p=0.315). **H)** Increased TIMP-2 immunoreactivity around D1 dendritic segments under extinguished conditions compared to SAL and RST (Nested 1-way ANOVA; $F_{(2,9)}$=7.20; p=0.014). **c)** Increased TIMP-1 and **I/J)** TIMP-2 immunoreactivity around D2 dendritic segments during cued heroin seeking (Nested 1-ANOVA; TIMP-1, $F_{(2,9)}$=19.08; p=0.001; TIMP-2, $F_{(2,71)}$=17.63; p<0.001). TIMP-1 and −2 expression was elevated around D2 MSNs during heroin seeking compared to D1 MSNs (TIMP-1, Nested t-test; $F_{(1,6)}$=9.03; p=0.024; TIMP-2, Nested t-test; $F_{(1,47)}$=9.91; p=0.003). Data shown as mean ± SEM. N represents number of neurons quantified over number of animals in each condition. *p<0.05 compared to SAL, $^{+}$p<0.05 compared to EXT using Sidak post hoc test. Bar= 5 μm.